IEICE Proceeding Series

Bifurcation of Chaos and Density Spectrum of Inter-Spike-Intervals from Piecewise-Constant Spike Oscillator

Takahiro Aoki, Tadashi Tsubone

Vol. 1 pp. 840-843
Publication Date: 2014/03/17
Online ISSN: 2188-5079

2012 International Symposium on Nonlinear Theory and its Applications
NOLTA2012, Palma, Majorca, Spain, October 22-26, 2012

Bifurcation of Chaos and Density Spectrum of Inter-Spike-Intervals from Piecewise-Constant Spike Oscillator

Takahiro Aoki[†a)] and Tadashi Tsubone[†b)]

†Nagaoka University of Technology
1603–1, Kamitomioka, Nagaoka, Niigata, 940–2188, Japan
Email: [a)]s093095@stn.nagaokaut.ac.jp, [b)]tsubone@vos.nagaokaut.ac.jp

Abstract—In this study, we focus on a spike oscillator with chaotic motion governed by piecewise-constant vector field. The spike oscillator exhibits bifurcation of chaos referred to as distinguishing phenomena called "Island" which is chaos whose support of invariant measure is divided into union of subintervals in the domain of the return map. On the other hand, the oscillator generates various chaotic spike train. The density spectrum of inter-spike-intervals undergo a characteristic change depending on the parameters, that is, bifurcation phenomena on density spectrum is observed. This paper derives an existence region of Island and shows the bifurcation set of chaos on a parameter space and density spectrum analytically. Almost complete analysis of bifurcation phenomena on density spectrum of inter-spike-intervals is provided.

1. Introduction

Recently, chaotic spike oscillators (abbr. CSOs) have been studied intensively in the field of nonlinear problem and neuroscience [1]-[5]. These CSOs have rotate-and-fire dynamics and the dynamics is analogous with some simple spike neuron models [6]. The CSOs behave chaotic oscillation and produce output pulse signals, i. e. spike, when the state variables of CSOs reach spiking thresholds. The spike elicits resetting operation of state variables. By these chaotic oscillation with the reset dynamics, CSOs exhibit various chaotic spike train. To study the spike train is not only interesting for basic problems of nonlinear systems but also important for applications based on neural systems and for pulse based communication systems [7]-[10].

In this research, we consider a piecewise-constant chaotic spike oscillator (abbr. PWCCSO) [11] and its frequency density of inter-spike-intervals (abbr. ISIs). PWCCSOs have attracted interest as a simple model of analog spike neurons because they can be implemented by simple nonlinear elements and can be set up the parameters easily due to its simplicity [12]. In addition, it is easy to theoretical analysis with regard to stability and bifurcation phenomena by using mapping procedure [3][11].

First, we consider bifurcation of chaos such that structure of chaotic attractor is transformed by changing parameters. The dynamics of a proposed PWCCSO can be reduced to one-dimensional (1-D) return map. We show the system exhibits remarkable bifurcation phenomena called "Island" which is chaos whose support of invariant measure is divided into union of subintervals in domain of the 1-D return map [13][14]. We emphasize that the bifurcation of chaos is caused by some kind of border collision bifurcation relevant to an unstable periodic orbit and an interior border embedded in chaos attractor.

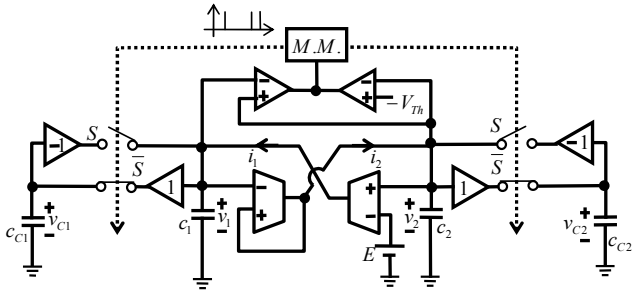

Figure 1: A chaotic spike oscillator.

Next, we focus on frequency density of ISIs and its bifurcation. Due to there are not many researches of the density spectrum of ISIs [15], analysis of global bifurcation for distribution spectrum of ISIs is challenging subject. We show the relationship between bifurcation of chaos and change of the distribution of ISIs using the return map.

We provide almost complete analysis of bifurcation phenomena both of on Island and on density spectrum of ISIs.

2. A chaotic spike oscillator with piecewise-constant vector field

Figure 1 shows a circuit model of a system. The triangles labeled 1 (-1, respectively) are linear amplifiers with gain 1 (-1, respectively). The triangles labeled "+ $-$" are comparators. These amplifiers and comparators are realized by operational amplifiers with sufficiently large input impedance. Trapezoids are differential voltage-controlled transconductance amplifiers and their output currents are i_1 and i_2, respectively. They are characterized by

$$\begin{aligned} i_1 &= I_a \cdot \mathrm{sgn}(v_2 - E) \\ i_2 &= I_a \cdot \mathrm{sgn}(v_2 - v_1) \end{aligned}, \quad \left(\mathrm{sgn}(x) = \begin{cases} 1 & \text{for } x \geq 0 \\ -1 & \text{for } x < 0 \end{cases} \right), \qquad (1)$$

where v_1 and v_2 are voltages across the capacitors C_1 and C_2, respectively. I_a is a constant current which is controlled

by a bias current of the transconductance amplifiers. When S is opened, the circuit dynamics is described by

$$\begin{aligned} \dot{x} &= \mathrm{sgn}(y-1), \\ \dot{y} &= \mathrm{sgn}(y-ax), \end{aligned} \tag{2}$$

where "$\cdot$" represents the derivative of normalized time τ and the following dimensionless variables and parameters are used.

$$\tau = \frac{I_a}{C_2 E}t,\ x = \frac{C_1}{C_2 E}v_1,\ y = \frac{1}{E}v_2,\ a = \frac{C_2}{C_1},\ Th = \frac{1}{E}V_{Th}. \tag{3}$$

Here, we assume the following parameter condition:

$$a > 1. \tag{4}$$

In this parameter range, Equation (2) has unstable rect-spiral trajectories as shown in Fig. 2. The trajectory on the phase space moves around the singular point $(\frac{1}{a}, 1)$ divergently and it must reach to the half line $l_{Th} = \{(x, y)|y = ax, y < -Th\}$ as shown in the left figure of Fig. 2. In the circuit in Fig. 1, *M.M.* is a monostable multivibrator which outputs pulse signals to close the switch S and to open $\bar{S}$ instantaneously. Two comparators detect the instantaneous switching condition. If $v_2 \le v_1$ or $v_2 \ge -V_{Th}$, the switch S is opened and $\bar{S}$ is closed. For the meantime, the voltage v_1 and v_2 are stored to C_{C1} and C_{C2}, respectively. If $v_2 > v_1$ and $v_2 < -V_{Th}$, then *M.M.* is triggered by the pair of comparators, and the switch S is closed and $\bar{S}$ is opened instantaneously. At that time, the voltage v_1 and v_2 are reset instantaneously to the inverse voltages $-v_1$ and $-v_2$, respectively. That is,

$$\begin{aligned} &[v_1(t^+), v_2(t^+)]^T = [-v_1(t), -v_2(t)]^T \\ &\quad \text{for } v_2(t) > v_1(t) \text{ and } v_2(t) < -V_{Th}, \end{aligned} \tag{5}$$

where $t^+ \equiv \lim_{\varepsilon \to 0}\{t + \varepsilon\}$.

Because of the parameter condition (4), the trajectory must reach $l_v \equiv \{(v_1, v_2)|v_2 = v_1, v_2 < -V_{Th}\}$ when the switching occurs. Namely, the normalized trajectory must hit l_{Th}, and jumps from $(x(T_n), y(T_n))$ to $(-x(T_n), -y(T_n))$ as shown in the left figure of Fig. 2, where T_n is the n-th switching moments.

Consequently, Eqn. (2) and (5) with the condition (4) are transformed into

$$\begin{aligned} &\begin{cases} \dot{x} = \mathrm{sgn}(y-1), \\ \dot{y} = \mathrm{sgn}(y-ax), \end{cases} \quad \text{for } S = \text{off}, \\ &[x(\tau^+), y(\tau^+)]^T = [-x(\tau), -y(\tau)]^T \\ &\quad \text{for } y(\tau) > a \cdot x(\tau) \text{ and } y(\tau) < -Th. \end{aligned} \tag{6}$$

Now the system is characterized by only two parameters a and Th. The right figure of Fig. 2 shows a typical chaotic attractor with $a \simeq 5.84$ in laboratory. The transconductances are implemented by operational transconductance amplifiers (abbr. OTAs) NJM13700. Realization procedure of differential voltage-controlled transconductance amplifiers by using OTAs can be found in literature [3]. The monostable multivibrator, the comparators and the analog switches are implemented by IC package of 4538, LM339 and 4066, respectively.

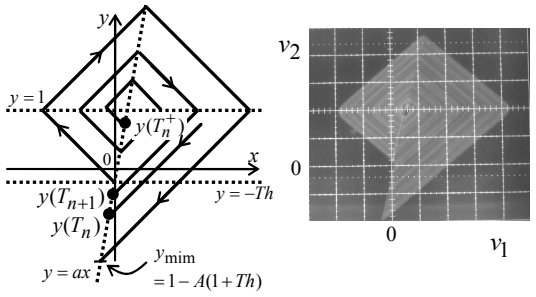

Figure 2: Behavior of trajectories on the phase space and a typical chaos attractor, $a \simeq 5.84$, vertical axis: 1[V/div.] and horizontal axis: 5[mV/div.] for right column.

3. Bifurcation of chaos

First of all, we derive embedded return map of the system. The exact piecewise solution of Eqn. (6) for S =off can be depicted as piecewise-linear trajectories. Here, let us focus on a trajectory starting from intersection point of $y = ax$ and $y = -Th$ at $\tau = 0$ (see Fig. 2). The trajectory rotates divergently around the singular point $(\frac{1}{a}, 1)$ and reaches the switching threshold. A y-coordinate of the reaching point is obtained as $1 - (\frac{a+1}{a-1})^2(1 + Th)$. Here let $A = (\frac{a+1}{a-1})^2$ and let $y_{\min} = 1 - A^2(1 + Th)$. We define $l = \{(x, y)|y_{\min} < y < -Th, y = ax\}$ and assume the case of $y_{\min} > -1$, that is, the minimum value of y is greater than -1. In this case, the trajectory starting from l must jump instantaneously to the symmetric point of the origin and rotates k-times $(k = 1, 2, 3, \cdots)$ around the singular point. Finally it must return to l. We henceforth consider the following parameter range with (4):

$$1 < A \le \frac{2}{1 + Th}. \tag{7}$$

If we choose l as Poincaré-section, we can define 1-D return map f from l to itself. Letting $(x(T_n), y(T_n))$ be the starting point, $(x(T_{n+1}), y(T_{n+1}))$ be the returning point as shown in the left figure of Fig. 2. Letting any points on l be represented by its y-coordinate, f is defined by

$$f : l \mapsto l, \quad y_{n+1} = f(y_n), \tag{8}$$

where we rewrite $y_n = y(T_n)$. Using piecewise-linear trajectories and linear algebraic procedure, we obtain an explicit expression for the function f.

$$f(y_n) = \begin{cases} f_1(y_n) = -A(y_n + 1) + 1 \\ \qquad \text{for } Th_1 < y_n \le Th_0, \\ f_2(y_n) = -A^2(y_n + 1) + 1 \\ \qquad \text{for } Th_2 < y_n \le Th_1, \\ \qquad \vdots \\ f_k(y_n) = -A^k(y_n + 1) + 1 \\ \qquad \text{for } Th_k < y_n \le Th_{k-1}, \\ \qquad \vdots \\ \qquad (k = 1, 2, 3, \cdots), \end{cases} \tag{9}$$

where each borders of the piecewise maps, $Th_k = \frac{1}{A^k}(1 + Th) - 1$ $(k = 1, 2, 3, \cdots)$, are derived by solving $-Th = -A^k(Th_k + 1) + 1$. And let $Th_0 = -Th$. Typical shapes of map f are shown in Fig. 3. Note that the branch of f_k corresponds to a trajectory with a k-turn spiral on the phase space. That is, the unstable fixed point P_k which satisfies $P_k = f_k(P_k)$ corresponds to a k-winding unstable periodic orbit (abbr. UPO).

Here, we give the proof for chaos generation of this system. From condition (7), $|\frac{\partial f}{\partial y_n}| > 1$ is satisfied almost everywhere without discontinuous points and $f(I) \subseteq I$ is obvious, hence f exhibits chaos on the condition (7). In practice, if $0 < Th < \frac{2}{A-\sqrt{A}} - 1$ and $A > 1$ is satisfied, the system (6) must behave chaos rigorously. This paper omits the proof but it is easy in a similar way to [3].

In the system (6), we can observe remarkable phenomena. Figure 4 shows chaotic attractors on the parameter $A = 1.16$ and $Th = 0.07$. Snapshot on left column is laboratory measurement and figure on right column indicates corresponding return map. The band which consists of 2-winding trajectories is separated into at least two 2-winding components. In this case, the support of invariant measure of the corresponding return map is divided into at least two parts and a blank region appears on domain of f_2 as shown in right figure of Fig. 4. Note that the blank region contains a unstable fixed point P_2.

This phenomenon is called "Island" and the sufficient condition for existence of k-Island is given by

$$f_{k+1}(y_{\min}) < P_k < f_{k-1}(Th_0). \tag{10}$$

Figure 5 shows existence regions of k-Island as I_k framed by two borders B_{kN} and B_{kP} which are obtained by solving $P_k = f_{k+1}(y_{\min})$ and $P_k = f_{k-1}(Th_0)$, respectively. A behavior on B_{kP} means that the trajectory started from an edge of attractor Th_0 hits k-winding UPO and a behavior on B_{kN} means that the trajectory started from an edge $y_{\min}$ hits the UPO. Since the trajectories started from the edge are some kind of borders in the interior of attractor, these behaviors on B_{kN} or B_{kP} can be considered as border collision bifurcation of UPO. Namely, Island appears or disappears on B_{kN} or B_{kP} due to occurrence of interior border collision of UPO. Although there are more Islands exist in I_k on Fig. 5, the existence region are quite narrow and method of analysis is almost the same as above. So, this paper omits the result.

4. Probability density of inter-spike intervals and its bifurcation

First, we derive the relationship function $T(y_n)$ between the inter-spike interval $\Delta\tau = T_{n+1} - T_n$ and the state y_n at the moment when a spiking occurs. If the trajectory hits the threshold l at $\tau = T_n$, a spiking occurs and the time interval until next spiking is determined uniquely by y_n. By using return map (8) and linear algebraic procedure, we obtain

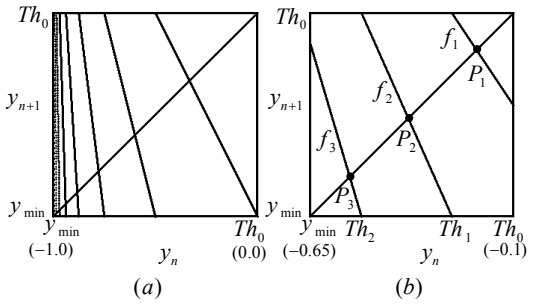

Figure 3: Chaotic return maps. (a): $Th = 0, A = 2(a \simeq 5.84)$, (b): $Th = 0.1, A = 1.5$.

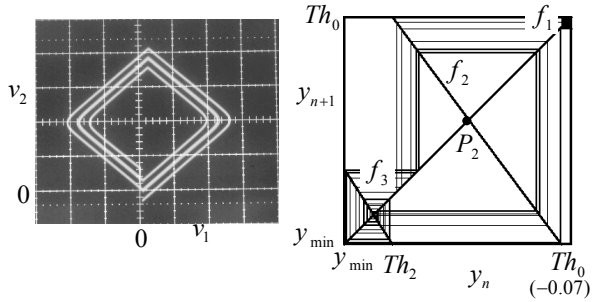

Figure 4: Bifurcation of chaos. $(A = 1.16, Th = 0.07)$, vertical axis: 1[V/div.] and horizontal axis: 5[mV/div.] for left figure.

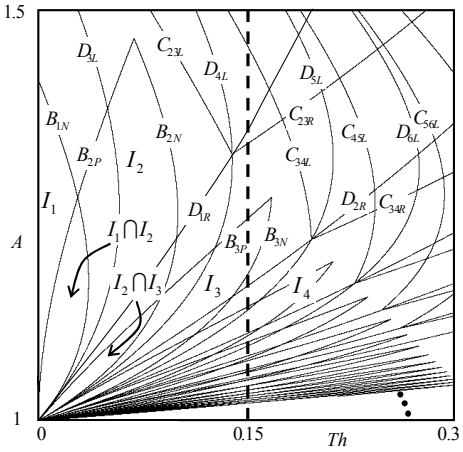

Figure 5: Bifurcation diagram for Islands and density spectrums of ISI.

the expression for the function $T(y_n)$.

$$\Delta\tau = T(y_n) = \begin{cases} (1 + y_n)(1 + \sqrt{A})^2 \\ \quad \text{for } Th_1 < y_n \le Th_0, \\ (1 + y_n)(1 + \sqrt{A})^2(1 + A) \\ \quad \text{for } Th_2 < y_n \le Th_1, \\ \quad \vdots \\ (1 + y_n)(1 + \sqrt{A})^2 \sum_{j=0}^{k-1} A^j \\ \quad \text{for } Th_k < y_n \le Th_{k-1}, \\ \quad \vdots \\ \quad (k = 1, 2, 3, \cdots), \end{cases} \tag{11}$$

Bottom right figure of Fig. 6(a) depicts an example of function $T(y_n)$ on $A = 1.2$ and $Th = 0.07$. If the invariant measure of the return map has been given, we can obtain directly the frequency density of ISI $p(\Delta\tau)$ by using the function $T(y_n)$;

$$p(\Delta\tau) = \int_{-1}^{0} \left(\frac{\partial \Delta T(y_n)}{\partial y_n} \right)^{-1} \delta(y_n, y_T) h(y_n) dy, \qquad (12)$$

where y_T is all values such as $\Delta\tau = T(y_T)$, $\delta(i, j)$ is Kronecker delta function and $h(y_n)$ is the density of the invariant measure of return map.

The bottom left figure of Fig. 6(a) shows histogram obtained by 100,000 sampled data of a numerical simulation. The range of value of T_2, T_3 and T_4 are separated each other on $T(y_n)$ and a segment of 3-turn trajectory is divided into two parts by 3-Island. So, distribution divided into some segments. Figure 6(b) shows bifurcation diagram of ISI distribution that is expressed by gray scale image. Such phenomena are caused by three types of bifurcation factors. (i) Appearance and extinguishing of a segment corresponding to k-turn trajectories. Existence condition of k-turn trajectories is given by $y_{\min} < Th_{k-1}$ and $Th_k < Th$. The borders D_{kL} and D_{kR} shown in Fig. 5 are given by solving $y_{\min} < Th_{k-1}$ and $Th_k < Th$, respectively. (ii) Unification and separation of two segments corresponding to k- and $k+1$-turn trajectories. These two segments separate when $T_{k+1}(y_{\min}) \geq T_k(Th_{k-1})$ or $T_{k+1}(Th_{k+1}) \geq T_k(Th_0)$ are satisfied. The bifurcation sets $C_{k,k+1L}$ and $C_{k,k+1R}$ are given by solving $T_{k+1}(y_{\min}) = T_k(Th_{k-1})$ and $T_{k+1}(Th_{k+1}) = T_k(Th_0)$, respectively. (iii) Generation and disappearance of Island considered in previous section.

These bifurcation sets are shown in Fig. 5.

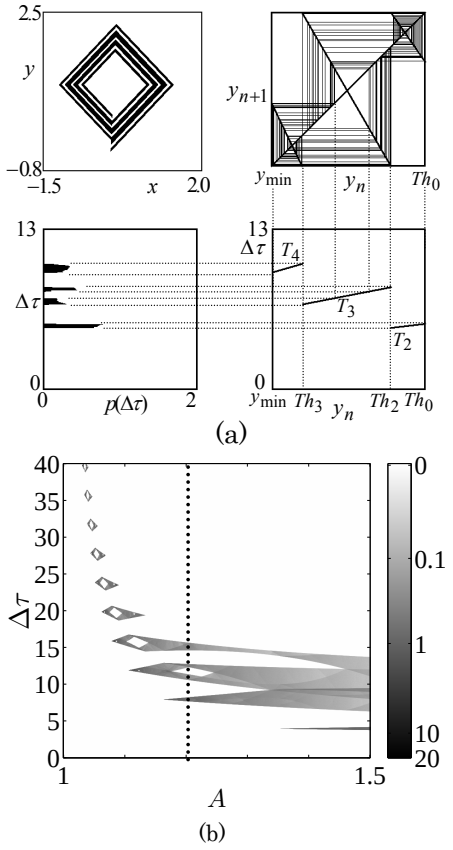

Figure 6: Bifurcation of frequency density of ISI ($Th = 0.15$). (a) Separation of distribution spectrums on $A = 1.2$. (b) Bifurcation diagram of frequency density of ISI.

5. Conclusion

We considered bifurcation phenomena on density spectrum of inter-spike-intervals of spikes which are generated from a spike oscillator with chaotic motion governed by piecewise-constant vector field. We derived existence regions of Island and the bifurcation sets of chaos on parameter space and density spectrum of inter-spike-intervals (ISI) using the return maps and relationship functions between state and ISI. Future works are more detailed verifications in laboratory and control bifurcation of distribution of ISI.

References

[1] K. Mitsubori and T. Saito, IEEE Trans. Circuit Syst. I, vol. 44, no. 12, pp. 1122–1128, Dec. 1997.

[2] H. Nakano and T.Saito, IEICE Trans. Fundamentals., vol. E84–A, no. 5, pp. 1293–1300, May. 2001.

[3] T. Tsubone and Y. Wada, IEICE Trans. Fundamentals., vol. E82–A, no. 5, pp. 1316–1321, May. 2009.

[4] T. Hishiki and H. Torikai, IEEE Trans. NN, vol. 22, no. 5, pp. 752–767, May. 2011.

[5] Y. Matsuoka, IEICE Trans. Fundamentals., vol. E94–A, no. 9, pp. 1860–1863, Sep. 2011.

[6] E. M. Izhikevich, "Dynamical Systems in Neuroscience," MIT Press, 2006.

[7] H. Nakano and T. Saito, IEEE Trans. NN, vol. 15, no. 5, pp. 1018–1026, Sep. 2004.

[8] H. Torikai and T. Nishigami, IEICE Trans. Fundamentals., vol. E92–A, no. 8, pp. 2053–2060, Aug. 2009.

[9] S. Hashimoto and H. Torikai, IEEE Trans. Circuit Syst. I, vol. 57, no. 8, pp. 2168–2181, Aug. 2010.

[10] P. Chiang and C. Hu, IEEE Trans. Circuit Syst. II: Express Briefs, vol. 57, no. 8, pp. 642–646, Aug. 2010.

[11] T. Tsubone and T. Saito, IEICE Trans. Fundamentals., vol. E82–A, no. 8, pp. 1619–1626, Aug. 1999.

[12] Y. Yamashita and H. Torikai, Proc. of IEEE-INNS/IJCNN'2011, pp. 717–724, Aug. 2011.

[13] S. Ito, S. Tanaka, and H. Nakada, Tokyo J. of Math., Vol. 02, No. 2, pp. 221-239, 1979.

[14] T. Saito, IEEE Trans. Circuit Syst. I, vol. 32, no. 4, pp. 320–331, April 1985.

[15] Y. Matsuoka, T. Hasegawa and T. Saito, IEICE Trans. Fundamentals., vol. E92–A, no. 4, pp. 1142–1147, Apr. 2009.